STRUCTURE OF IONIC LIQUIDS AND IONIC LIQUID COMPOUNDS: ARE IONIC LIQUIDS GENUINE LIQUIDS IN THE CONVENTIONAL SENSE?

HIRO-O HAMAGUCHI and RYOSUKE OZAWA

Department of Chemistry, School of Science, The University of Tokyo, Tokyo, Japan

CONTENTS

I. INTRODUCTION

The term *ionic liquid* (IL) refers to a class of liquids that are composed solely of ions. It is a synonym of molten salt. Although molten salt implicitly means a high-temperature liquid that is prepared by melting a crystalline salt, IL includes a new class of ionic compounds that are liquids at the ambient temperature [1]. Thus, IL in a narrow sense often stands for room-temperature ionic liquid (RIL). In the present chapter, IL is used in a broader sense and, if necessary, RIL is used to clarify that it is liquid at the ambient temperature. The history of ILs has already been reviewed [2].

Advances in Chemical Physics, Volume 131, edited by Stuart A. Rice

In contrast to ordinary molecular liquids, in which the dipolar and/or higher-order multipolar electrostatic interactions are dominating, the Coulomb interaction plays a major role in ILs. It is well known that the long-range nature of the Coulomb interaction makes the melting points of ionic crystals much higher than those of molecular crystals. In that sense, RILs are somewhat extraordinary; the melting point of a typical RIL, 1-butyl-3-methyl-imidazolium iodide, is −72°C [3], while a typical ionic crystal NaI melts only at 651°C. Here, we have the most fundamental and profound question about RIls. Why are RIls liquids at the ambient temperature, despite the fact that they are composed solely of ions? A few important questions then follow. Are there any liquid structures that are characteristic of the dominating Coulomb interactions in RILs? Will there be any novel properties that originate from those specific structures of RILs? In order to answer these questions, we need to elucidate the structure and dynamics of RILs and related IL compounds.

In spite of these basic interests of high importance, the structural studies of Ils are scant and are still in a developing stage. Most of the IL studies so far are directed toward their possible applications [4–6]. The high-temperature stability, nonvolatility, nonflammablility, amphiphilicity, and many other characteristics of RILs as solvents are potentially useful as a new class of "Green" solvents. The wide potential window (large difference in the oxidation and reduction potentials) of ILs promises applications as new electrochemical materials. New types of catalysts based on Ils have also been explored [7]. Under these circumstances, it is not possible to provide a perspective overview on the structure and dynamics of Ils in general. We therefore focus here on the structural studies on Ils having the imidazolium-based cations—in particular, the Raman spectroscopic and x-ray studies carried out in the past few years. Thus, the present chapter is more like an advances report rather than a comprehensive review. The authors hope that it would nevertheless be helpful to the many researchers who are coming into the wonder world of ionic liquids.

The 1-butyl-3-methylimidazolium cation, $bmim^+$ (Fig. 1), makes a number of ILs with varying properties, when combined with different anions [4]. BmimCl and bmimBr are crystals at room temperature, while bmimI is a RIL. By cooling down molten bmimCl and bmimBr below the melting points, their

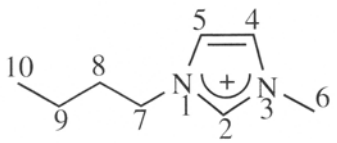

Figure 1. The 1-butyl-3-methylimidazolium cation, $bmim^+$.

supercooled liquids are easily obtained. Those halogen salts thus comprise a unique system for studying the structure of the $bmim^+$ cation in the crystalline and liquid states at room temperature. X-ray diffraction can determine the structures in crystals, while Raman spectroscopy facilitates comparative studies of the structures in crystals and liquids. The two salts, bmim[BF_4] and bmim[PF_6], are prototype RILs that are most extensively used in basic IL investigations as well as in practical applications. Therefore, the elucidation of the crystal and liquid structures of the $bmim^+$-based Ils will be an important first step for the understanding of ILs in general.

In the following, we first discuss the crystal polymorphism of bmimCl and the crystal structures of bmimCl and bmimBr. The results of single crystal x-ray analysis are given to show that the crystal polymorphism is due to the *trans–gauche* rotational isomerism of the butyl group of the $bmim^+$ cation. They also show that the cations and the halogen anions in bmimCl and bmimBr crystals separately form characteristic column structures extending along the crystal *a* axis. Then, comparison of the Raman spectra and the normal coordinate analysis lead to a conclusion that at least two rotational isomers, one having a *trans* conformation and the other having a *gauche* conformation with regard to the C_7–C_8 bond of the butyl group of the $bmim^+$ cation, coexist in the ionic liquid state. A few pieces of experimental evidence are then given which are indicative of some local structures existing in ILs. The unusual long equilibration time between the *trans* and *gauche* conformers upon melting of a small single crystal of the *trans* polymorph of bmimCl indicates that the rotational isomers do not interconvert with each other at the molecular level. The two rotational isomers are most likely to be incorporated in their specific local structures, and they can interconvert with each other only through the conversion of the local structure as a whole. The apparent enthalpy differences between the *trans* and *gauche* conformers in a group of 1-alkyl-3-methylimidazolium tetrafluoroborate ILs are much smaller than the corresponding enthalpy difference between the *trans* and *gauche* conformers of the free alkyl chain. This finding also indicates that the 1-alkyl-3-methylimidazolium cation form local structures specific to each rotational isomers. Coexistence of these local structures incorporating different rotational isomers may well hinder crystallization and hence lower the melting points of the 1-alkyl-3-methylimidazolium based ILs. The wide-angle x-ray scattering results on bmimI IL show prominent peaks in the residual radial distribution curve, indicating certain periodical arrangements of the iodide anions. These local structures, if they exist, distinguish ILs from the conventional molecular liquids. It is argued that ILs may form an entirely new material phase that exists in between liquid and crystal. These local structures may also lead to unique properties of ionic liquids. For example, if magnetic anions are aligned in ILs, novel magnetic liquids will be created.

II. CRYSTAL POLYMORPHISM OF bmimCl

Crystal polymorphism of bmimCl was reported almost simultaneously by two groups [8, 9]. We found by chance that two different types of crystals, Crystal (1) and Crystal (2), formed when liquid bmimCl was cooled down to −18°C and was kept for 48 h [8]. Orthorhombic Crystal (2) dominantly formed but monoclinic Crystal (1) also formed occasionally (see Fig. 2).

Upon leaving Crystal (2) for more than 24 h at dry-ice temperature, Crystal (2) was converted to Crystal (1). It is not clear yet whether Crystal (1) forms directly from the liquid state or not. Holbrey et al. [19] independently obtained two crystal polymorphs, orthorhombic Crystal I and monoclinic Crystal II. Crystal I was obtained by cooling down slowly the molten liquid to room temperature, while Crystal II was obtained by cooling ionic liquid mixtures, bmimCl/bmim[PF_6] and bmimCl/bmim[BF_4]. Crystal II was also obtained by crystalization from a hexane–benzene mixed solvent. The melting points of Crystals I and II measured by DSC were reported by Holbrey et al. to be 66°C and 41°C, respectively. Independent DSC measurements by us [10] showed somewhat different results. Crystal (1) melted at varying temperature in the range between 47°C and 67°C depending on individual crystals, although single crystals were used for the DSC measurements. Crystal (2) melted at 64°C. The DSC curves of the two polymorphs showed broad melting peaks as also mentioned by Holbrey et al. These extraordinary DSC behaviors are indicative of complex structure and dynamics of bmimCl Crystal1 (1) with regard to the temperature change. From the crystal types and the melting points,

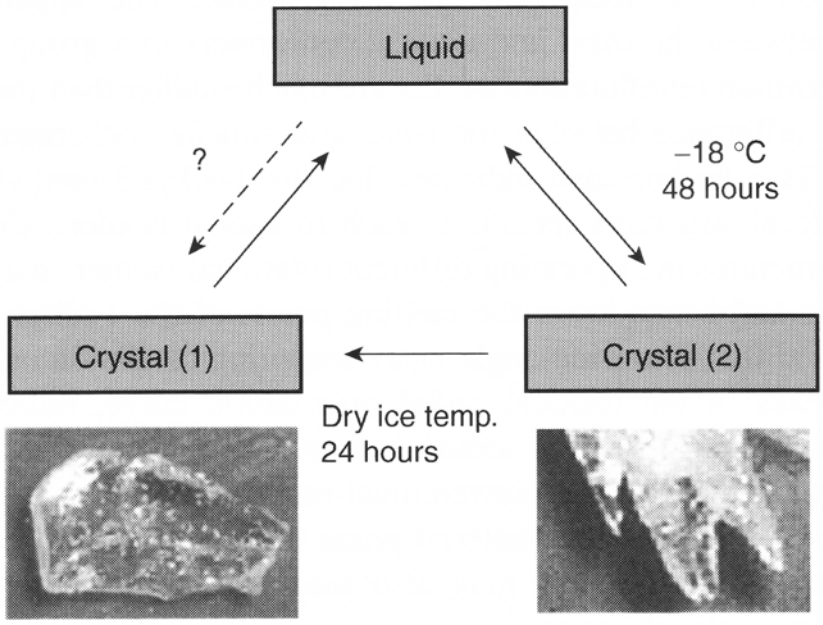

Figure 2. Crystal polymorphism of bmimCl.

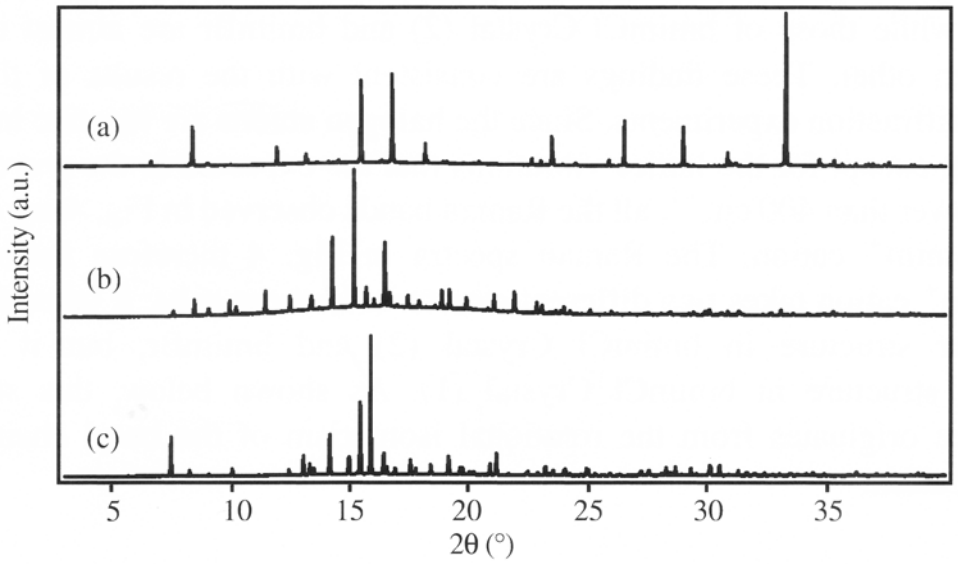

Figure 3. X-ray powder diffraction patterns of (*a*) bmimCl Crystal (1), (*b*) bmimCl Crystal (2), and (*c*) bmimBr.

it is obvious that Crystal I corresponds to Crystal (2) and Crystal II to Crystal (1). In the following, we use the notation Crystal (1) and Crystal (2).

The x-ray powder diffraction patterns of bmimCl Crystal (1) and (2) are shown in Fig. 3 [8]. The sharp peaks with distinct patterns indicate that they are different crystals and that neither of them is an amorphous solid. The continuous background notable for Crystal (2) is most likely to arise from the structural disorder existing in the crystal. The x-ray powder diffraction pattern of bmimBr is also shown in Fig. 3 for comparison. The pattern of bmimBr is more close to that of bmimCl Crystal (2) than to Crystal (1).

The Raman spectra of bmimCl Crystals (1) and (2), and that of bmimBr, are compared in Fig. 4 [8]. The polymorphs of bmimCl give two distinct Raman

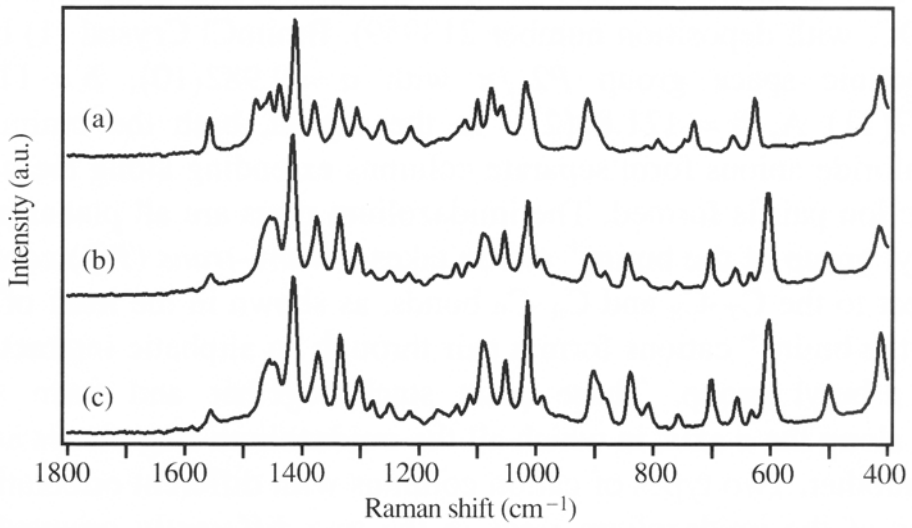

Figure 4. Raman spectra of (*a*) bmimCl Crystal (1), (*b*) bmimCl Crystal (2), and (*c*) bmimBr.

spectra, while those of bmimCl Crystal (2) and bmimBr are almost identical with each other. These findings are consistent with the results of the x-ray powder diffraction experiments. Since the halogen anions are inactive in Raman scattering except for the lattice vibrations that are expected in the wavenumber region lower than 400 cm^{-1}, all the Raman bands observed in Fig. 4 are ascribed to the $bmim^+$ cation. The Raman spectra in Fig. 4 therefore indicate that the $bmim^+$ cation takes two different structures in those salts; it takes the same molecular structure in bmimCl Crystal (2) and bmimBr, but it takes a different structure in bmimCl Crystal (1). As shown below, this structural difference originates from the rotational isomerism of the butyl chain of the $bmim^+$ cation.

III. CRYSTAL STRUCTURES OF bmimCl CRYSTAL (1) AND bmimBr

Subsequent to the discovery of the crystal polymorphism of bmimCl, the crystal structures of bmimCl and bmimBr were determined. We determined the crystal structures of bmimCl Crystal (1) and bmimBr at room temperature [11, 12]. Independently, Holbrey et al. [9] reported the crystal structures of bmimCl Crystal (1) and Crystal (2), as well as that of bmimBr at $-100°C$. The two sets of structures determined at different temperatures agree well with each other except for the lattice constants that vary with temperature. They also show that the molecular structure of the $bmim^+$ cation in bmimCl Crystal (2) is different from that in (1) but that it is the same as that in bmimBr, as already indicated by the Raman spectra. In the following, we discuss the crystal structures of bmimCl Crystal (1) and bmimBr as the two representative structures at room temperature.

The crystal structure of bmimCl Crystal (1) is shown in Fig 5. The detailed structural data are available from the Cambridge Crystallographic Data Centre [12] (CCDC, with deposition number 213959). BmimCl Crystal (1) belongs to the monoclinic space group $P2_1/n$ with $a = 9.982(10)$, $b = 11.590(12)$, $c = 10.077(11)$ A, $\beta = 121.80(2)°$. In the crystal, both the $bmim^+$ cations and the chloride anions form separate columns extending along the a axis, and no specific ion pair is formed. The imidazolium rings are all planar pentagons. The n-butyl group of the $bmim^+$ cation takes a *trans–trans* (TT) conformation with respect to the C_7–C_8 and C_8–C_9 bonds, as shown in the inset of Fig. 5. A couple of the $bmim^+$ cations form a pair through an aliphatic interaction of the stretched n-butyl group. Those pairs stack together and form a column extending along the a axis, in which all the imidazolium ring planes are parallel with one another. Two types of cation columns with different orientations exist. The planes of the imidazolium rings in the two differently oriented columns make an angle of 69.5°. A zigzag chain of the anion Cl^- directed in the a

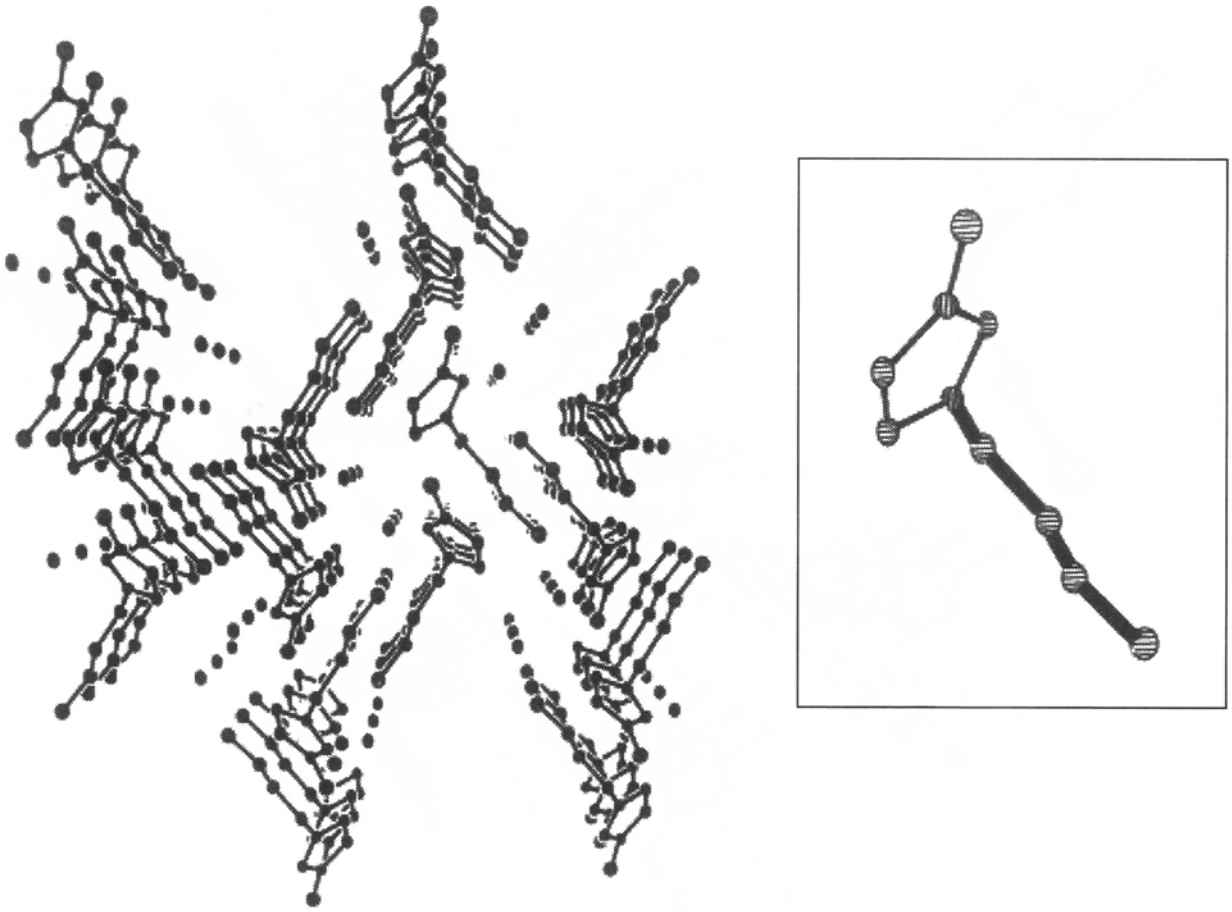

Figure 5. Crystal structure of bmimCl Crystal (1) viewed over the *a* axis. Carbon atoms, nitrogen atoms, and chloride anions are shown. The *trans–trans* conformation of the butyl group of the $bmim^+$ cation is shown in the inset with the relevant C–C bonds marked by thick bars.

direction (Fig. 6) are accommodated in a channel formed by four cation columns, of which two opposite columns have the same orientation. The shortest three distances between Cl^- anions in the zigzag chain are $r_1 = 4.84$ Å, $r_2 = 6.06$ Å, and $r_3 = 6.36$ Å. These distances are much larger than the sum of the van der Waals radii of Cl^- (3.5 Å). There seems to be no specific interactions among the Cl^- anions, and they are likely to be aligned under the

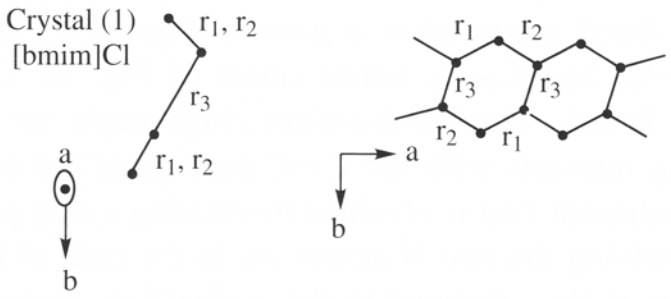

Figure 6. The zigzag structure of chloride anions in bmimCl Crystal (1).

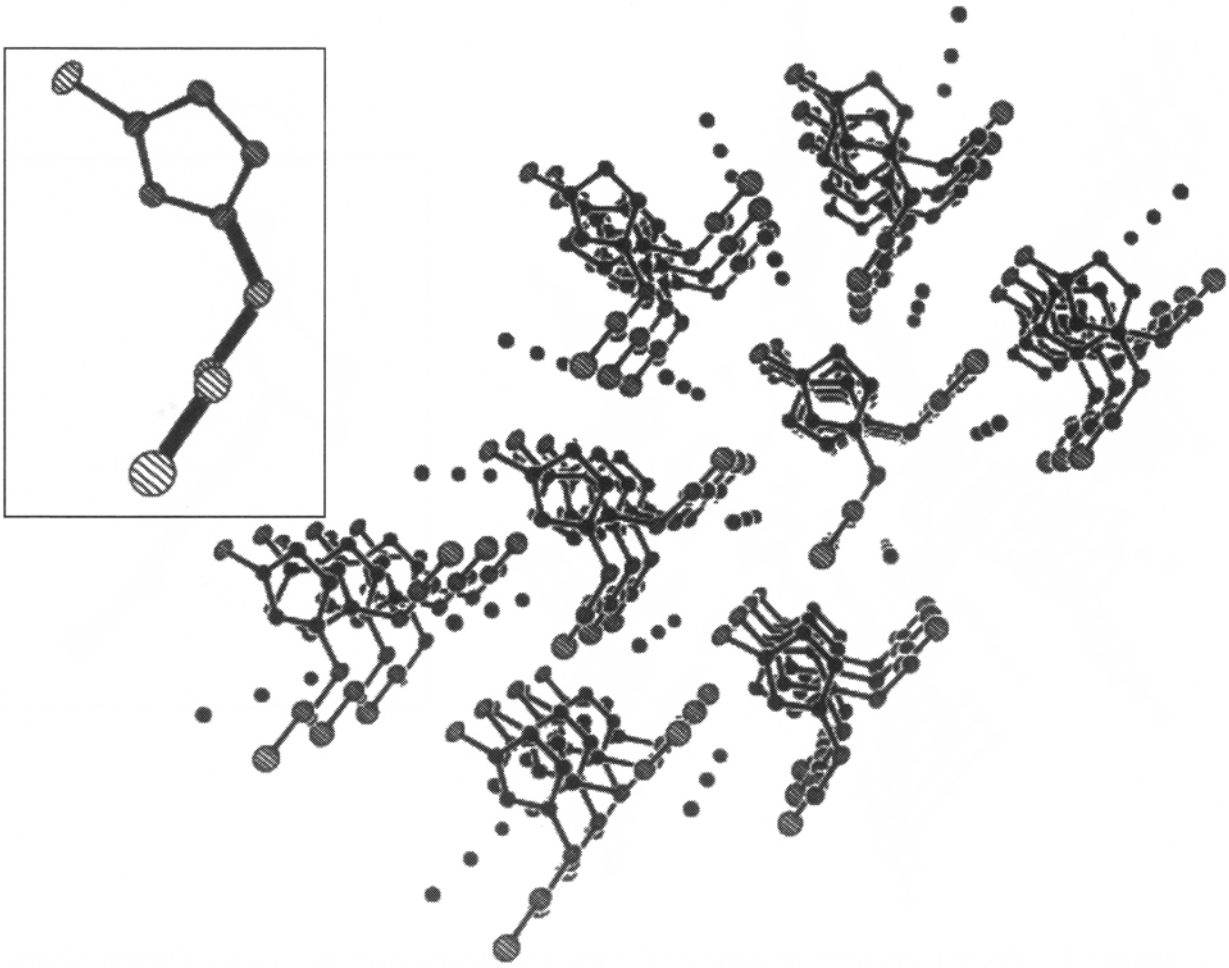

Figure 7. Crystal structure of bmimBr viewed in the direction of the *a* axis. Carbon atoms, nitrogen atoms, and bromide anions are shown. The *gauche–trans* conformation of the butyl group of the $bmim^+$ cation is shown in the inset with the relevant C–C bonds marked by thick bars.

effect of the Coulomb force. Similar crystal structures were also reported for 1-ehtyl-3-methylimidazolium chloride (emimCl) [13].

The molecular arrangements in a crystal of bmimBr are shown in Fig. 7. Detailed crystal data are registered as CCDC 213960. BmimBr belongs to the orthorhombic space group $Pna2_1$ with $a = 10.0149(14)$, $b = 12.0047(15)$, $c = 8.5319(11)$ A. As in the case of bmimCl Crystal (1), the $bmim^+$ cations and the halogen anions form separate columns extending along the *a* axis and no ion pairs exist. The *n*-butyl group takes a *gauche–trans* (*GT*) conformation with respect to the C_7–C_8 and C_8–C_9 bonds (inset of Fig. 8). Only one kind of cation column is found. The imidazolium rings stack so that the N–C–N moiety of one ring interacts with the C=C portion of the adjacent ring. The orientation of the adjacent ring is obtained by rotating a ring plane by about 73° around an axis involving the two N atoms. As in the case of [bmim]Cl Crystal (1), a zigzag chain of Br^-, directed in the *a* direction, is accommodated in a channel produced by four cation columns, which are also extending in the *a*

direction. The shortest three Br^-–Br^- distances are 4.77, 6.55, and 8.30Å and are all longer than the sum of the van der Waals radii (3.7 Å). This fact again indicates that there are no specific interactions among the Br^- anions and that they are arranged in the zigzag form as a result of the Coulomb interaction.

IV. NORMAL MODE ANALYSIS AND ROTATIONAL ISOMERISM OF THE $Bmim^+$ CATION

The Raman spectral variations of the $bmim^+$ cation in bmimX crystals (Fig. 4) are interpreted very well in terms of the rotational isomerism of the butyl group. Figure 8 compares the Raman spectra of bmimCl Crystal (1) and bmimBr in the wavenumber region of 400–1000 cm^{-1}. The structures of the $bmim^+$ cation in the two crystals are also depicted in the same figure.

In the wavenumber region 600–700 cm^{-1}, where ring deformation bands are expected, two bands appear at 730 cm^{-1} and 625 cm^{-1} in bmimCl Crystal (1)

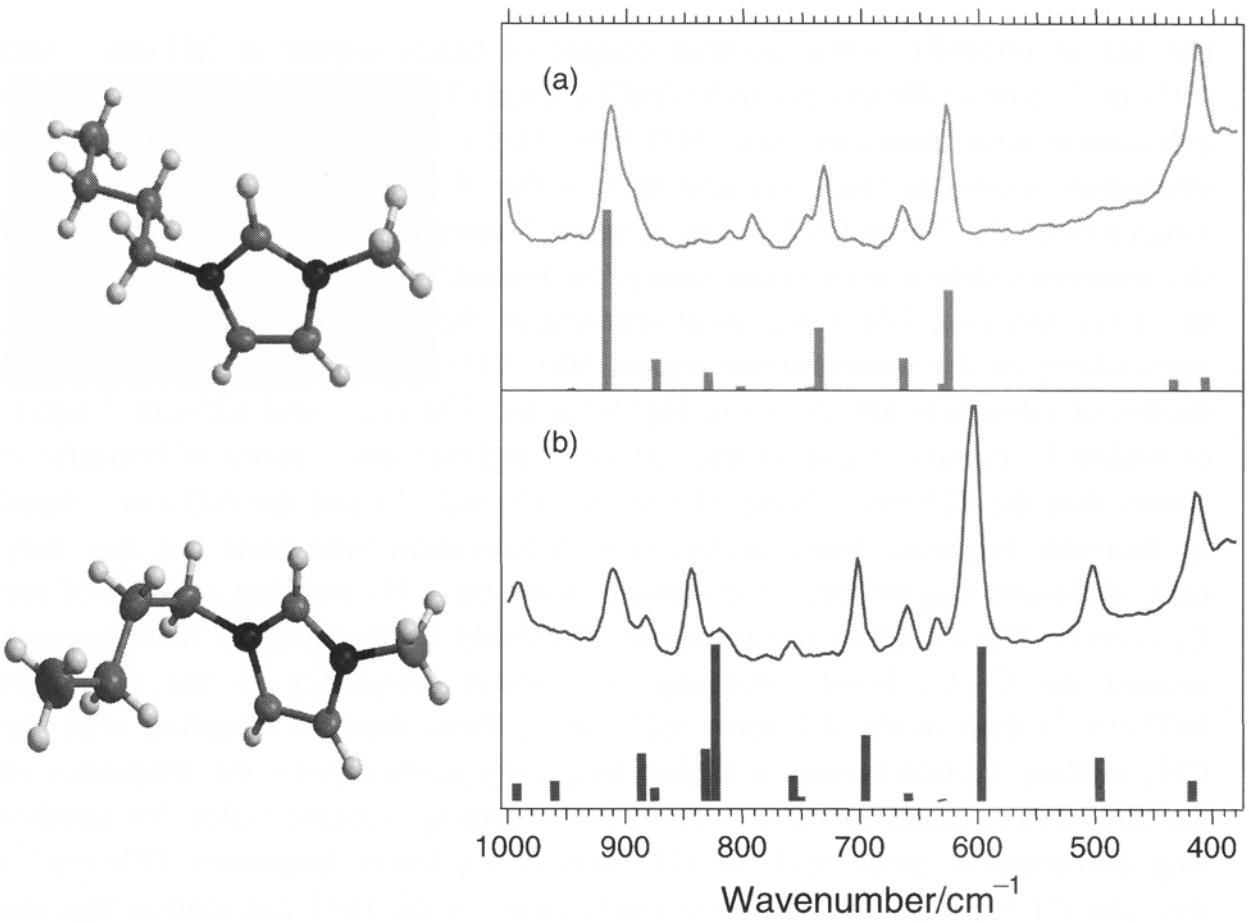

Figure 8. Raman spectra of (*a*) bmimCl Crystal (1) and (*b*) bmimBr. The structures of the $bmim^+$ cation in the two crystals are depicted on the right-hand side. The thick vertical bars indicate calculated frequencies and Raman intensities.

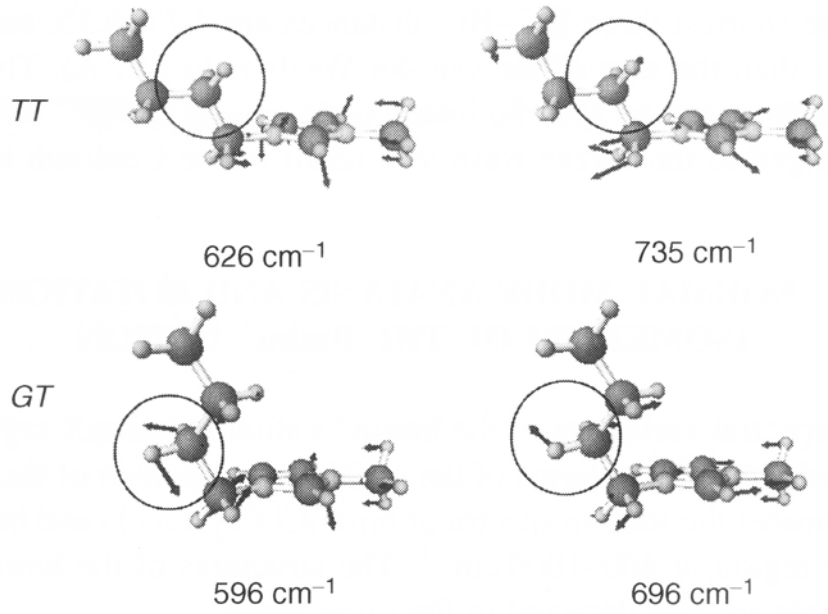

Figure 9. Calculated normal modes of the two key bands of the TT and GT forms of the $bmim^+$ cation. The arrows indicate vibrational amplitudes of atoms. The CH_2 rocking vibration of the C_8 methylene group are surrounded by a circle.

but not in bmimBr, while another couple of bands appear at 701 cm^{-1} and 603 cm^{-1} in bmimBr and not in bmimCl crystal (1). A DFT (density functional) calculation with Gaussian 98(6), B3LYP/6-31G+** level gives frequencies and intensities shown as thick vertical bars in Fig. 9 [14]. In this calculation, the structures of the *TT* and *GT* forms of $bmim^+$ were optimized in the vicinity of the structures determined, respectively, for bmimCl Crystal (1) and bmimBr by the x-ray analysis. The calculation reproduces the observed spectra very well, particularly in the wavenumber region 500–700 cm^{-1}. The calculated normal modes of vibrations are shown in Fig. 9 for the 730-cm^{-1} and 625-cm^{-1} bands of bmimCl Crystal (1) and for the 701-$cm^{-1}$and 603-cm^{-1} bands of bmimBr. It shows that the 625-cm^{-1} band of bmimCl Crystal (1) and the 603-cm^{-1} band of bmimBr originate from similar ring deformation vibrations but that they have different magnitudes of couplings with the CH_2 rocking motion of the C_8 carbon. The coupling occurs more effectively for the *gauche* conformation around the C_7–C_8 bond, resulting in a lower frequency in the *GT* form (603 cm^{-1}) than in the *TT* form (625 cm^{-1}). Note that the coupling with the CH_2 rocking motion having a higher frequency pushes down the frequency of the ring deformation vibration. The same coupling scheme holds for another ring deformation mode and the *GT* form has a lower frequency (701 cm^{-1}) than the *TT* form (730 cm^{-1}). It is made clear by the DFT calculation that the 625-cm^{-1} and 730-cm^{-1} bands are characteristic of the *trans* conformation around the C_7–C_8 bond, while the 603-cm^{-1} and 701-cm^{-1} bands are characteristic of the *gauche* conformation. In other words, we can use these

bands as key bands to probe the conformation around the C_7–C_8 bond of the $bmim^+$ cation.

V. RAMAN SPECTRA AND LIQUID STRUCTURE OF BmimX

With the structural information obtained from the crystals, we are now in a position to discuss the liquid structure of bmimX ionic liquids. Raman spectra of liquid bmimX (X = Cl, Br, I, BF_4, PF_6) are shown in Fig. 10. The Raman spectra of bmimCl Crystal (1) and bmimBr are also shown as references. All Raman spectra were measured at room temperature. The Raman spectra of liquid bmimCl and bmimBr were obtained from their supercooled states.

The Raman spectra of the BF_4^- and PF_6^- anions are already well known. Except for these anion bands that are deleted in Fig. 10, the Raman spectra of liquid bmimX are surprisingly alike with one another. It seems that the structure of the $bmim^+$ cation is very similar in these liquids. Both of the two sets of key bands, the 625-cm^{-1} and 730-cm^{-1} bands for the *trans* conformation and the 603-cm^{-1} and 701-cm^{-1} bands for the *gauche* conformation, appear in all of the

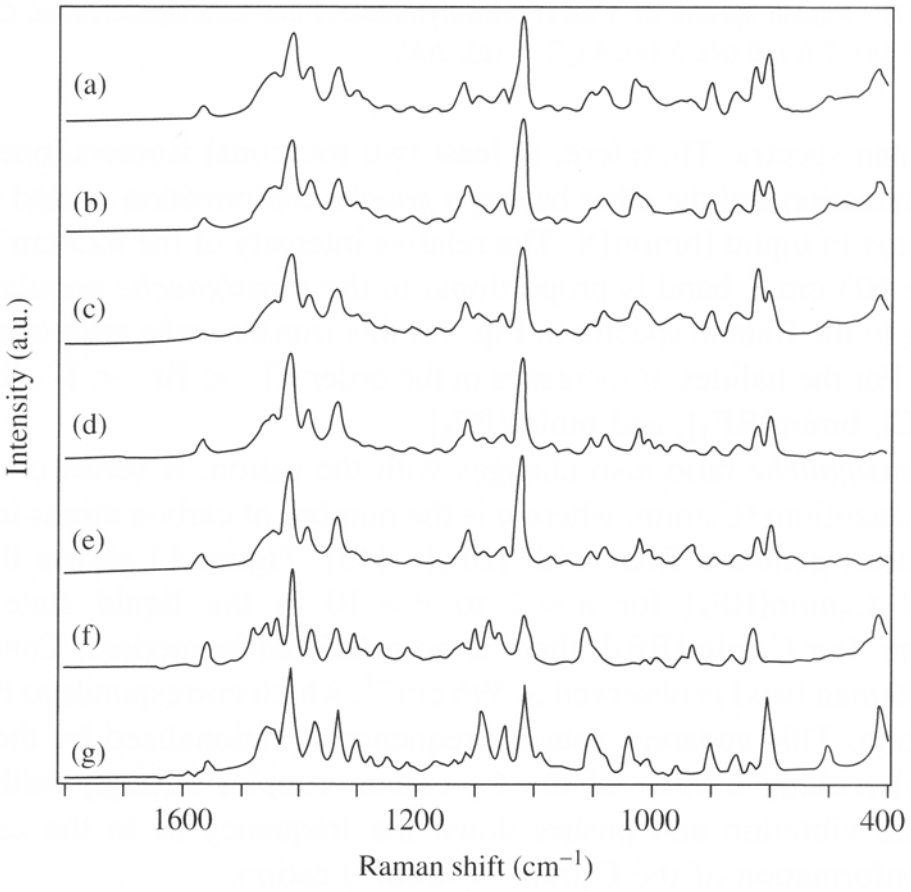

Figure 10. Raman spectra of liquid bmimX, where X = Cl (*a*), Br (*b*), I (*c*), [BF4] (*d*), and [PF6] (d). The anion bands in (d) and (*e*) are deleted. Raman spectra of bmimCl Crystal (1) and that of crystalline bmimBr are also shown as references in (*f*) and (*g*), respectively.

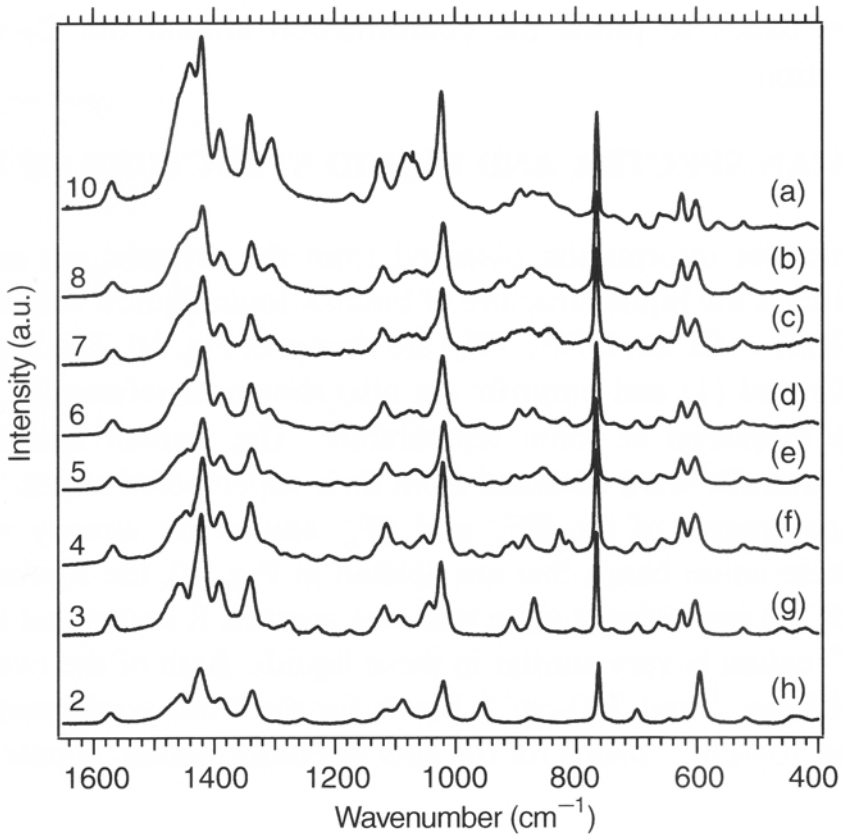

Figure 11. Raman spectra of 1-alkyl-3-methylimidazolium tetrafuluoroborate, $C_n$mim[BF_4]; $n = 10$ (*a*), 8 (*b*), 7 (*c*), 6 (*d*), 5 (*e*), 4 (*f*), 3 (*g*), 2(*h*).

liquid Raman spectra. Therefore, at least two rotational isomers, one having a *trans* conformation and the other having a *gauche* conformation around the C_7–C_8 bond, coexist in liquid [bmim]X. The relative intensity of the 625-cm^{-1} band to that of the 603-cm^{-1} band is proportional to the *trans/gauche* population ratio. According to the Raman spectra in Fig. 10, this *trans/gauche* ratio changes with the anion. For the halides, it increases in the order $Cl^- < Br^- < I^-$. It is similar for bmimCl, bmim[BF_4], and bmim[PF_6].

The *trans/gauche* ratio also changes with the cation. A series of 1-alkyl-3-methylimidazolium ($C_n$mim, where n is the number of carbon atoms in the alkyl chain) cations generate RILs with $[BF_4]^-$ [15]. Figure 11 shows the Raman spectra of $C_n$mim[BF_4] for $n = 2$ to $n = 10$ in the liquid state at room temperature. For C_2mim[BF_4], there is no rotational isomerism. Consequently, only one Raman band is observed at 596 cm^{-1}, which corresponds to the *gauche* conformation. This apparent gauche frequency is rationalized by the fact that the methyl rocking motion of the C_8 carbon couples strongly with the ring deformation vibration and pushes down the frequency as in the case of the *gauche* conformation of the C_4mim^+ ($bmim^+$) cation.

For the carbon number larger than two ($n > 2$), the 625/603-cm^{-1} Raman intensity ratio increases with increasing n. The *trans* band at 625 cm^{-1} is weaker in intensity than the *gauche* band at 603 cm^{-1} for $n = 3$, but the

intensity ratio is reversed for $n = 10$. Since the vibrational modes giving rise to those bands are very similar with each other and localized within the imidazolium ring and the C_7 and C_8 carbons (see Fig. 9), their Raman cross sections are thought to be independent of the chain length. Therefore, the 625/603-cm^{-1} Raman intensity ratio can be regarded as a direct measure of the *trans/gauche* isomer ratio. The observed increase of the 625/603-cm^{-1} Raman intensity ratio then means that the *trans/gauche* isomer ratio increases as the chain becomes longer. In other words, the *trans* structure is stabilized relatively to the *gauche* for longer alkyl chains. Such stabilization of the *trans* isomer is understandable only if we assume interactions among the cations. Otherwise, the relative stability is determined by the energy difference (about 0.6 kcal/mol [16]) between the *trans* and *gauche* conformations around the C_7–C_8 bond and is more likely to be independent of the chain length. We know from the crystal structure of C_4mimCl (bmimCl) Crystal (1) that a couple of C_4mim^+ cations make a pair through an aliphatic interaction between the two alkyl groups. The chain-length dependence of the *trans/gauche* ratio is thus indicative of an interaction between two $C_n$mim cations, most probably through an aliphatic interaction between the two alkyl chains. In Fig. 11, broad Raman features are observed for longer-chain $C_n$mim[BF_4] ($n = 7$–10) in the wavenumber region of 800–950 cm^{-1}, where the rocking and the other hygrogen bending vibartion of the methylene groups are located. These broad features are also indicative of a specific interaction between the alkyl chains. The crystal structures of $C_n$mimCl and $C_n$mim[PF_6] show interdigitated structures of alkyl groups when $n > 12$ [17–19]. Similar interdigitated structures of alkyl chains are also suggested in the meso-phase of $C_n$mimCl ($n = 12$–18) [20].

VI. POSSIBLE LOCAL STRUCTURES IN BmimX IONIC LIQUIDS

The interaction through the alkyl chains is likely to operate also in bmimX ILs. In fact, there are more experimental results that strongly suggest the interaction among the cations and the formation of local structures in bmimX ILs. First, unusually long equilibration time between the *trans* and *gauche* conformers has been observed for liquid bmimCl [21]. A small piece (0.5 mm × 0.5 mm × 0.5 mm) of [bmim]Cl crystal (1) was heated abruptly with a heat gun from room temperature to 72°C, and a droplet of liquid in a nonequilibrium state was transiently formed. The sample was then kept at 72°C to get thermally equilibrated. The time-resolved Raman spectra in Fig. 12 show this melting and equilibration processes. Before melting, only the *trans* band at 625 cm^{-1} is observed in the 600- to 630-cm^{-1} region, reflecting the *trans* structure of the $bmim^+$ cation in Crystal (1). Immediately after melting, the 625-cm^{-1} band remains much stronger than the *gauche* band at 603 cm^{-1}. Then, the *gauche* band

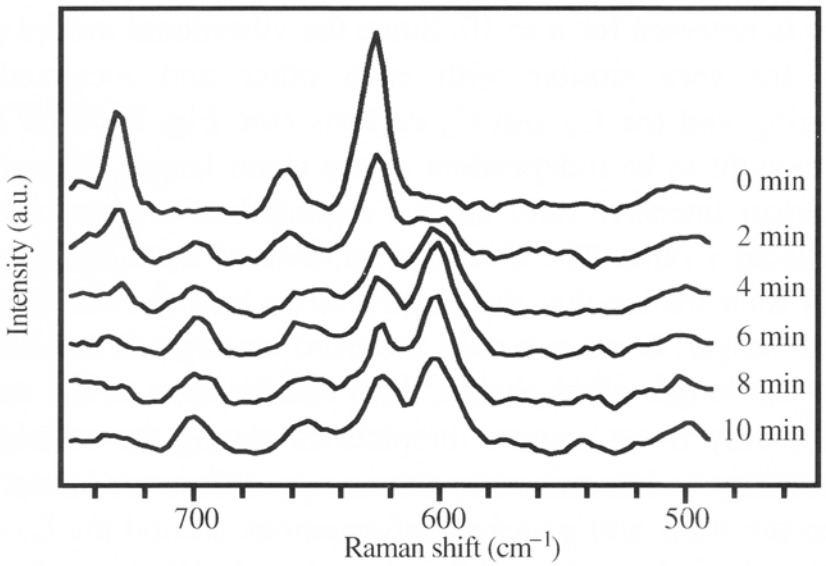

Figure 12. Time-resolved Raman spectra of the melting and thermally equilibration process of bmimCl Crystal (1).

becomes stronger as time goes on, and the *trans/gauche* intensity ratio becomes constant after 10 min. Thus, it takes about 10 min for the *trans* and *gauche* conformers in liquid bmimCl to get thermally equilibrated. If the $bmim^+$ cation undergoes the *trans/gauche* transformation at the single molecular level, as expected for a free butyl chain, the equilibration should occur instantaneously. Note that the *trans* and *gauche* isomers of alkyl chains are not separately observed but give a coalesced peak in NMR spectra, indicating that transformation between them takes place much faster than a second. The observed unusually long equilibration time, 10 min, therefore indicates that the *trans* and *gauche* conformers of $bmim^+$ in liquid bmimCl are not transformed from each other at the single molecular level but that they can be interconverted only through a slow collective transformation (analogous to phase transition) of the ensembles of $bmim^+$ cations. It is most probable that the two rotational isomers are incorporated in their specific local structures and that they can interconvert with each other only through the conversion of those local structures as a whole.

The idea of different local structures incorporating the *trans* and *gauche* conformers is also consistent with the observed enthalpy differences. Table I gives the enthalpy differences ($\Delta H = H_{gauche} - H_{trans}$) between the *gauche* and *trans* conformers in the $C_n mim[BF_4]$ system determined from the temperature dependence of the Raman intensity ratio of the 625-cm^{-1} and 603-cm^{-1} bands [22]. As shown in the table, the determined enthalpy difference is very small for $n = 4, 5$, and 6, meaning that the two isomers are associated with almost the same enthalpy. It becomes the largest for $n = 10$. It is known that the ΔH value for a free alkane chain is around 0.6 kcal/mol [16]. However, all the obtained ΔH values for $C_n mim[BF_4]$ are significantly smaller than 0.6 kcal/mol. This disagreement is explained well in terms of the local structure formation of

TABLE I
The Apparent Enthalpy Difference Between the *trans* and *gauche* Conformers for $C_n$mim[BF_4] [22]

n	ΔH (kcal mol^{-1})	Melting Point (°C) [15]	Glass Transition Temperature (°C) [15]
3	−0.1	—	−13.9
4	0.01	—	−71.0
5	0.02	—	−88.0
6	−0.01	—	−82.4
8	0.09	—	−78.5
10	0.19	−4.2	—

the $C_n$mim cations; the determined enthalpy differences are associated with the alkyl chains incorporated in the local structures and not with those for free alkane chains. The dependence of the enthalpy difference on the chain length is also of considerable interest. For $n = 3$–8, for which the magnitude of the ΔH values are smaller than 0.1, no liquid/crystal transitions are observed and the glass state is formed form the liquid [15]. Only for $n = 10$, for which ΔH is significantly larger than those of the others, a clear melting point is reported. This trend suggests that the coexistence of the two different local structures, which incorporate the *trans* and *gauche* conformers of the $bmim^+$ cation and have similar enthalpies, hinders crystallization and hence lowers the melting points (liquid/glass transition temperature) of $C_n$mim[BF_4] with $n = 3$–8.

The ordering of the anions in bmimX ionic liquids has also been suggested by our recent large-angle x-ray scattering experiment on liquid bmimI [23]. Figure 13 shows a differential radial distribution function obtained for liquid bmimI at room temperature. Clear peaks in the radial distribution curve are

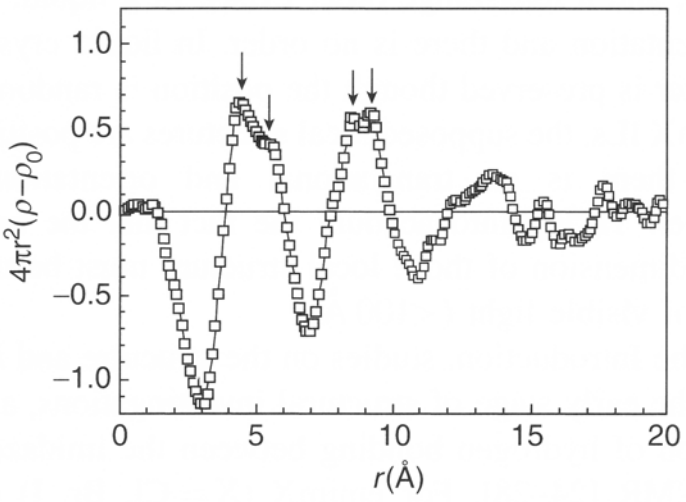

Figure 13. Differential radial distribution function of liquid bmimI by large-angle x-ray scattering [23].

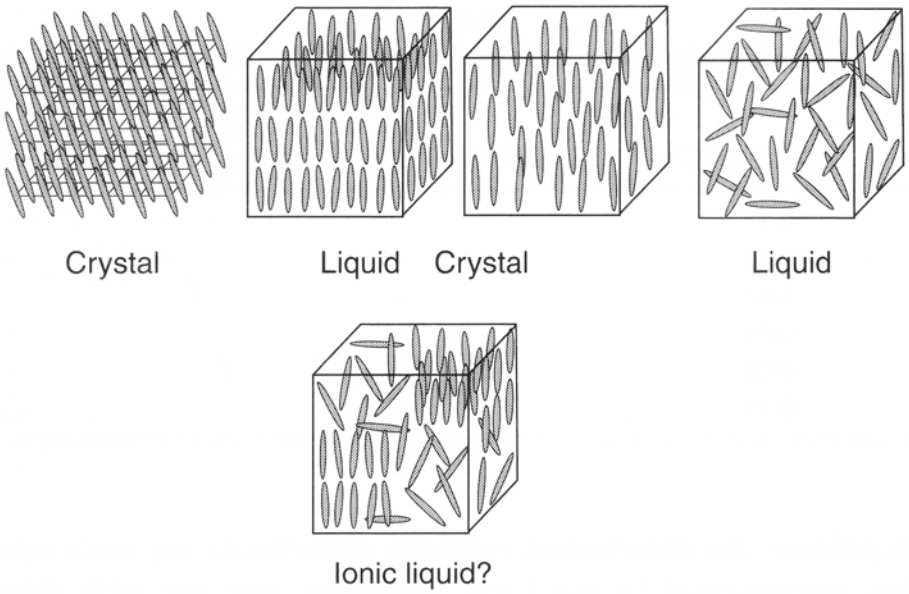

Figure 14. Conceptual structure of an ionic liquid.

observed at 4.5, 5.5, 8.5, and 9.2 Å (arrows in Fig. 14). The shortest distance, 4.5 Å, corresponds very well to the shortest halogen–halogen distance found in the crystal structures of bmimCl Crystal (1)(4.84 Å) and bmimBr (4.65 Å). The other distances can also be correlated to the other halogen–halogen distances in the zigzag chains shown in Fig. 6. It seems that the zigzag chains found in the bmimX crystals do exist, at least partially, and may be in a slightly distorted form, in the ionic liquid state as well.

In this way, by combining several pieces of experimental evidence obtained so far, we come to a thought that both the cations and anions in bmimX ILs do have local ordering or structures. The conceptual structure of a bimimX IL is shown in Fig. 14 in comparison with the structures of a crystal, liquid crystals, and a liquid. In a crystal, component molecules or ions are periodically arranged to form a lattice, and a long-range order exists. In a liquid, they take random position and orientation and there is no order. In liquid crystals, a long-range orientational order is preserved though the position is random or only partially ordered. In bmimX ILs, the supposed local structures are positioned and oriented randomly, and there is no translational and orientational order in the macroscopic level. Taking into account the fact that the bmimX ILs are all transparent, the dimension of those local structure must be much smaller than the wavelength of visible light (<100 Å).

As stated in the Introduction, studies on the strucutre and interactions in ILs are limitted. In the early stage of structural investingations, a focus was placed on the elucidation of hydrogen bonding between the imidazolium cations and the anions by NMR [24–28]. For emimX (X = Cl, Br, I) diluted in several solvents, the formation of hydrogen bonding has been indicated between the cation and the anion via the hydrogen atoms attached to the C_2, C_4, and C_5

carbons [25]. From the measurement of the ^{13}C dipole–dipole relaxation rate, Huang et al. [26] have suggested that the hydrogen atom attached to the C_2 carbon participates in the hydrogen bonding with anions in neat emim[BF_4]. Similar results are also reported for bmim[PF_6] and bmim[BF_4] by Saurez et al. [27] and Lin et al. [28]. Interestingly, Saurez et al. suggest the existence of extended hydrogen-bonded networks at 279 K in bmim[BF_4]. The extended structure via hydrogen bonding is also suggested by Abdul-Sada et al. [29] for 1-alkyl-3-methylimidazolium halide by use of fast-atom bombardment mass spectroscopy. Recently, charge ordering in ILs is discissed by Hardacre et al. [30, 31]. They have obtained the radial distribution function of dimethylimidazolium chloride and dimethylimidazolium hexaflurophosphate using neutron diffraction and argued that there is significant charge ordering of ions and hence the local structures in ILs and that the local structure resembles that found in the solid state. The charge ordering is also discussed by computer simulation studies. A number of computer simulation studies have been conducted on 1-alkyl-3-methylimidazolium-based ILs in recent few years [32–41]. The radial distribution functions calculated in these articles give similar results, all suggesting the long-range charge ordering. These results, though reported fragmentally, give support to our idea that ILs are unique in that they have more ordering in structure than do conventional molecular liquids.

If local structures do exist in ILs as discussed above, many unique properties are expected to arise therefrom. In fact, unusually high viscosity of ILs is ascribable to the local structures that hinder the translational motion of the ions. Amphiphilicity of ILs is also well-explained in terms of the inhomogeneous nature of ILs having local structures; polar molecules are dissolved in a polar part composed of the cation centers and anions, while nonpolar molecules are accommodated in a nonpolar part where alkyl chains are densely located. One of the most interesting properties that are expected to arise from the local ordering of ions is the magnetism. If magnetic ions are locally aligned in a liquid and if the spin angular momenta of those ions are strongly interacting with one another, we may be able to have an unusual magnetic liquid. We recently demonstrated that bmim[$FeCl_4$] responds strongly to a magnet, as shown in Fig. 15. It turned out that this RIL was nearly paramagnetic with no strong interactions among the spins. By combining many different cations and

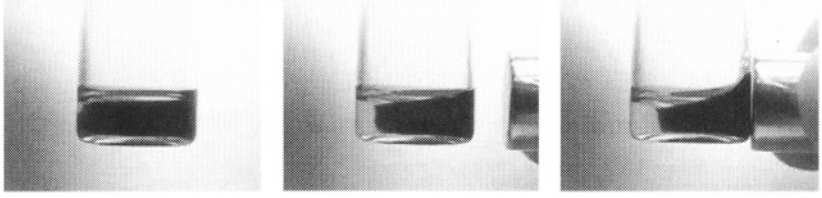

Figure 15. Pictures showing the response of bmim[$FeCl_4$] to a magnet [42].

magnetic anions, however, it may be possible to prepare superparamagnetic or even ferromagnetic ionic liquids in the near future.

VII. CONCLUSIONS

Raman spectroscopic and x-ray diffraction studies of bmimCl Crystal (1) and Crystal (2) and of crystalline bmimBr have revealed that two rotational isomers, the *trans–trans* and *gauche-trans* forms of the butyl group of the $bmim^+$ cation, exist in these crystals. Raman spectra and a DFT calculation show that at least two rotational isomers, one having a *trans* and the other having a *gauche* conformation around the C_7–C_8 bond of the butyl group, coexist in bmimX ionic liquids, where X = Cl, Br, I, BF_4,PF_6. Time-resolved Raman study of the melting and equilibration processes of bmimCl Crystal (1) suggests that the $bmim^+$ cations in those liquids form local structures that are specific to the *trans* and *gauche* conformers. It is likely that these local structures are similar to those found in the crystals. Coexistence of two different local structures, which incorporate the *trans* and *gauche* conformers separately, is likely to hinder crystallization of liquid bmimX and hence lower the melting points of the corresponding crystals. The size and the relaxation time of those local structures in bmimX ILs are yet to be elucidated, and they should be studied urgently in the nearest future.

If the local structure formation discussed in this chapter is not specific to bmimX ILs but applies to ILs in general, ILs may not be genuine liquids in the conventional sense. They might be better called **nano-structured fluid** or **crystal liquid**. They may form a new meso-phase that is distinct from the liquid crystal phase.

Acknowledgments

The authors are grateful to Mr. Satoshi Hayashi, Dr. Satyen Saha, Dr. Hideki Katayanagi, and Professor Keiko Nishikawa for collaboration.

References

1. K. R. Seddon, *J. Chem. Tech. Biotechnol.* **68**, 351 (1997).
2. J. S. Wilkes, *Green Chem.* **4**, 73 (2002).
3. J. G. Huddleston, A. E. Visser, W. M. Reichert, H. D. Willauer, G. A. Broker, and R. D. Rogers, *Green Chem.* **3**, 156 (2001).
4. T. Welton, *Chem. Rev.* **99**, 2071 (1999).
5. P. Wasserscheid and W. Keim, *Angew. Chem. Int. Ed.* **39**, 3772 (2000).
6. Saurez et al. *Chem. Rev.* **102**, 3667 (2002).
7. J. H. Davis, Jr, *Chem. Lett.* **33**, 1072 (2004).

8. S. Hayashi, R. Ozawa, and H. Hamaguchi, *Chem. Lett.* **32**, 498 (2003).
9. J. D. Holbrey, W. M. Reichert, M. Nieuwenhuyzen, S. Johnston, K. R. Seddon, and R. D. Rogers, *Chem. Commun.* 1636 (2003).
10. S. Wang, K. Tozaki, H. Katayanagi, H. Hayashi, H. Inaba, S. Hayashi, H. Hamaguchi, Y. Koga, and K. Nishikawa, to be published.
11. S. Saha, S. Hayashi, A. Kobayashi, and H. Hamaguchi, *Chem. Lett.* **32**, 740 (2003).
12. Cambridge Crystallographic Data Centre, http://www.ccdc.cam.ac.uk.
13. A. Elaiwi, P. B. Hitchcock, K. R. Seddon, N. Srinivasan, Y. M. Tan, T. Welton, and J. A. Zora, *J. Chem. Soc. Dalton Trans.*, 3467 (1995).
14. R. Ozawa, S. Hayashi, S. Saha, A. Kobayashi, and H. Hamaguchi, *Chem. Lett.* **32**, 948–949 (2003).
15. J. D. Holbrey and K. R. Seddon, *J. Chem. Soc., Dalton Trans.*, 2133 (1999).
16. (a) N. Shepard and G. J. Szasz, *J. Chem. Phys.* **17**, 86 (1949). (b) R. G. Snyder, *J. Chem. Phys.* **47**, 1316 (1947).
17. C. M. Gordon, J. D. Holbrey, A. R. Kennedy, and K. R. Seddon, *J. Mater. Chem.* **8**, 2627 (1998).
18. J. D. Roche, C. M. Gordon, C. T. Imrie, M. D. Ingram, A. R. Kennedy, F. L. Celso, and A. Triolo, *Chem. Mater.* **15**, 3089 (2003).
19. A. Downard, M. J. Earle, C. Hardcre, S. E. J. McMath, M. Nieuwenhuyzen, and S. J. Teat, *Chem. Mater.* **16**, 43 (2004).
20. A. E. Bladley, C. Hardcre, J. D. Holbrey, S. Johnston, S. E. J. McMath, and M. Nieuwenhuyzen, *Chem. Mater.* **14**, 629 (2002).
21. H. Hamaguchi, R. Ozawa, S. Hayashi, and S. Satyen. Abstract of Papers of the American Chemical Society, **226**, U622 (2003).
22. R. Ozawa, and H. Hamaguchi, to be published.
23. H. Katayanagi, S. Hayashi, H. Hamaguchi, and K. Nishikawa, *Chem. Phys. Lett.* **392**, 460–464 (2004).
24. W. R. Carper, J. L. Pflung, A. M. E. Elias, and J. S. Wilkes, *J. Phys. Chem.* **96**, 3828 (1992).
25. A. G. Avent, P. A. Chaloner, M. P. Day, K. R. Seddon, and T. Welton, *J. Chem. Soc. Dalton Trans.*, 3405 (1994).
26. J. F. Huang, P. Y. Chen, I. W. Sun, and S. P. Wang, *Inorg. Chim. Acta* **320**, 7 (2001).
27. P. A. Z. Suarez, S. Einloft, J. E. L. Dullius, R. F. Souza, and J. Dupont, *J. Chim. Phys.* **95**, 1626 (1998).
28. S. T. Lin, M. F. Ding, C. W. Chang, and S. S. Lue, *Tetrahedron* **60**, 9441 (2004).
29. A. K. Abdul-Sada, A. E. Elaiwi, A. M. Greenway, and K. R. Seddon, *Eur. Mass Spectrom.* **3**, 245 (1997).
30. C. Hardacre, S. E. J. McMath, M. Nieuwenhuyzen, D. T. Brown, and A. K. Soper, *J. Chem. Phys.* **118**, 273 (2003).
31. C. Hardacre, S. E. J. McMath, M. Nieuwenhuyzen, D. T. Brown, and A. K. Soper, *J. Phys. Condens. Matter.* **15**, 159 (2003).
32. C. G. Hanke, S. L. Price, and R. M. Lynden-Bell, *Mol. Phys.* **99**, 801 (2001).
33. J. K. Shah, J. F. Brennecke, and E. J. Maginn, *Green Chem.* **4**, 112 (2004).
34. T. I. Morrow and E. J. Maginn, *J. Phys. Chem. B* **106**, 12807 (2002).
35. J. D. Andrade, E. S. Böes, and H. Stassen, *J. Phys. Chem. B* **106**, 3546 (2002).

36. J. D. Andrade, E. S. Böes, and H. Stassen, *J. Phys. Chem. B* **106**, 13344 (2002).
37. C. J. Margulis, H. A. Stern, and B. J. Berne, *J. Phys. Chem. B* **106**, 12017 (2002).
38. M. G. D. Pópolo, and G. A. Voth, *J. Phys. Chem. B* **108**, 1744 (2004).
39. Z. Liu, S. Huang, and W. Wang, *J. Phys. Chem. B* **108**, 12978 (2004).
40. S. M. Urahata and M. C. C. Ribeiro, *J. Chem. Phys.* **120**, 1855 (2004).
41. J. K. Shah and E. J. Maginn, *Fluid Phase Equilibria* **195**, 222 (2004).
42. S. Hayashi and H. Hamaguchi, *Chem. Lett.* **33**, 1590 (2004).